ACS APPLIED MATERIALS & INTERFACES

www.acsami.org
Research Article

Microbial β-Glucuronidase Hydrogel Beads Activate Chemotherapeutic Prodrug

Yoon Jeong, Xiaoxue Han, Khushali Vyas, and Joseph Irudayaraj*

Cite This: ACS Appl. Mater. Interfaces 2024, 16, 28093−28103
Read Online

ACCESS | Metrics & More | Article Recommendations | Supporting Information

ABSTRACT: Bacteria-assisted chemotherapeutics have been highlighted as an alternative or supplementary approach to treating cancer. However, dynamic cancer−microbe studies at the *in vitro* level have remained a challenge to show the impact and effectiveness of microbial therapeutics due to the lack of relevant coculture models. Here, we demonstrate a hydrogel-based compartmentalized system for prodrug activation of a natural ingredient of licorice root, glycyrrhizin, by microbial β-glucuronidase (GUS). Hydrogel containment with *Lactococcus lactis* provides a favorable niche to encode GUS enzymes with excellent permeability and can serve as an independent ecosystem in the transformation of pro-apoptotic materials. Based on the confinement system of GUS expressing microbes, we quantitatively evaluated chemotherapeutic effects enhanced by microbial GUS enzyme in two dynamic coculture models *in vitro* (i.e., 2D monolayered cancer cells and 3D tumor spheroids). Our findings support the processes of prodrug conversion mediated by bacterial GUS enzyme which can enhance the therapeutic efficacy of a chemotherapy drug under dynamic coculture conditions. We expect our *in vitro* coculture platforms can be used for the evaluation of pharmacological properties and biological activity of xenobiotics as well as the potential impact of microbes on cancer therapeutics.

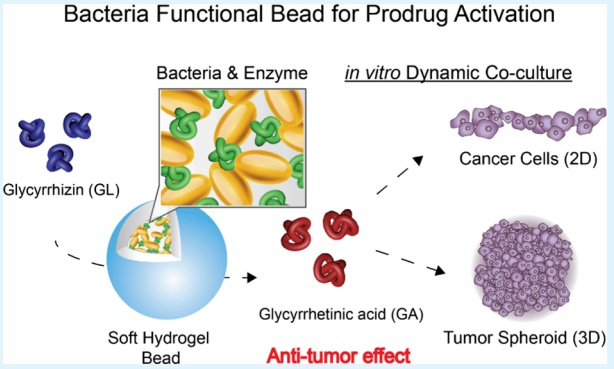

KEYWORDS: *prodrug activation, bacteria, cancer, tumor spheroid, hydrogel, β-glucuronidase, glycyrrhizin*

INTRODUCTION

Microorganisms are involved in a number of biological processes through the synthesis or breakdown of molecules contributing to bioavailability, chemical diversity, and biological activity of organisms in the environment.[1−5] Bacteria have a distinct feature to encode for various enzymes capable of processing endogenous metabolites and/or exogenous chemical compounds (e.g., pharmaceuticals, environmental chemicals, and other xenobiotics).[6−8] Numerous bacterial enzymes provide an important basis for physiological alteration or maintenance between organisms. Research on the interplay of bacteria and host cells in the context of drug efficacy in the host niches is a rapidly emerging field.[9,10]

Diverse species of engineered or attenuated wild-type bacteria (e.g., *Bifidobacterium* sp., *Vibrio cholerae*, *Clostridium difficile*, *Escherichia coli*, and *Salmonella* sp.) have been the subject of increased interest in translational oncology relating to drug administration.[11−13] In addition, the use of pro-apoptotic substances (i.e., prodrug) obtained from either natural sources or synthetic process have been studied by activating nontoxic and exogenous substances to cytotoxic compounds through bacteria-mediated transformation in various studies related to cancer.[14−18] Murine animal models are commonly used as test platforms for bacteria administration studies given the lack of relevant *in vitro* microbe−host interaction model systems.[19−21] Research efforts have focused on an effective delivery method for bacterial translocation and localization of chemotherapeutic activity at the site of the tumor. However, such procedures have remained a challenge because *in vivo* tumor−microbe treatments have not been standardized yet for microorganism-based treatment modalities.[22,23] Bacterial sustainability and high plasmid stability necessitate a favorable niche for their designed tasks. Furthermore, bacteria translocation and maintenance in the tumor microenvironment are not completely understood in relation to the mode of interaction with the host.

Designing multiscale *in vitro* studies with controllable experimental factors has been a challenge for the evaluation of pharmacological properties and biological activity of xenobiotics in microbial oncology. Current preclinical research relies heavily on *in vitro* studies due to the complex nature of

Received: February 14, 2024
Revised: May 8, 2024
Accepted: May 10, 2024
Published: May 22, 2024

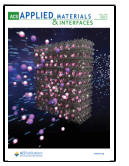

elucidating organism interaction.[24] A significant gap exists in a dynamic configuration of *in vitro* test platforms to assess interspecies interaction (i.e., bacteria and cancer cells). Besides, *in vitro* studies relating to bacteria-assisted therapy have not considered dynamic interactions between species.[25,26] Inactivated bacteria, bacterial extracts, exotoxins, or bacteria-free supernatant have been utilized as an alternative to evaluating indirect response of the host cancer cells *in vitro* due to uncontrollable growth or lack of standardized methods for cultivating specific bacteria.[22,27−30] Above all, the physiological state of microorganisms and their interactions in a dynamic coculture format will be important for bacteria maintenance, sustainability, and functionality. Despite advances in this field, a comprehensive understanding of the dynamic interaction at the interspecies level is lacking due to limitations in technology that can enable coculture studies on organisms of interest. Only a few techniques on dynamic coculture platforms exist to address the gap in this field.[25,27,31,32] To date, none of the dynamic cancer−microbe *in vitro* studies have assessed the impact and efficacy of microbial therapeutics for prodrug activation.

In this study, we explored bacteria-based prodrug activation to evaluate enhanced therapeutic effects on 2D cancer cells and 3D spheroid models to fill the gap in knowledge. Our previous efforts have suggested a hydrogel-based compartmentalized system for dynamic interspecies coculture studies to query bidirectional intra- and interspecies alterations.[33−35] Based on the conceived system, a probiotic *Lactococcus lactis* strain expressing β-glucuronidase (GUS) enzyme was encapsulated in a biofilm-like hydrogel bead. This *L. lactis* strain is widely used as a starter bacterium capable of producing specific enzymes in food, dairy, and health sectors.[36] In addition, bacterial GUS enzyme plays a central role in the biological processes associated with the hydrolyzation of glucuronic acid from glucuronides.[8,37] Suitably, a natural ingredient of licorice root, glycyrrhizin (also known as glycyrrhizic acid, GL), was assessed as a pro-apoptotic compound.[38] To demonstrate this concept, we established two experimental models to study this effect in a dynamic coculture format. The first constitutes the evaluation of cellular variations on 2D cancer cells cultured in monolayers, and the latter is the investigation of 3D tumor spheroid model; to assess whether a *GUS L. lactis* bacteria colonized in the hydrogen-shell structure can induce the enhanced therapeutic effect of a pro-apoptotic drug. We expect our *in vitro* coculture platforms utilizing tunable hydrogel beads with bacteria can avail new avenues in microbial oncology.

RESULTS AND DISCUSSION

Hydrogel Reaction System for Prodrug Activation. An artificial environment, composed of natural polysaccharide polymers, has long been used to entrap bacteria in a variety of biocontainment systems due to biofilm-like polysaccharide features of microbial origin. As depicted in Figure 1, the structure of the hydrogel core enclosed by an alginate-shell layer can act as a functional container to perform specific tasks. The hydrogel environment provides structural and functional integrity to render a favorable niche with excellent permeability and high growth density of entrapped bacteria as forming colonies.[34,39] (Figure S1) The bacterium selected for this study is *GUS* enzyme expressing *L. lactis* (*GUS L. lactis*) that can cleave the glucuronide moiety of pro-apoptotic drugs. When recapitulated in the hydrogel structure for sustenance, the *GUS*

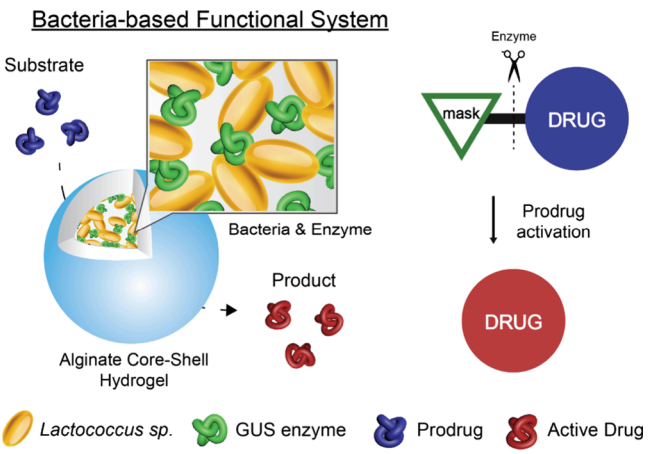

Figure 1. Bacteria-based enzymatic reaction systems to activate prodrug. Hydrogel-shell beads provide a biomimetic microenvironment for bacteria colonization with the synthesis of specific enzyme. The hydrogel biocontainment system with bacteria colonization and enzyme synthesis can act as a bioreactor for the conversion of prodrug to cytotoxic compounds.

L. lactis bacteria could balance proliferation and death to perform the designed tasks for prodrug activation by the secreted GUS enzyme. Thus, the living microbial hydrogel bead can serve as an independent bioreactor and play a role in the transformation of pro-apoptotic substances.[33]

The initial steps constitute the fabrication and characterization of an independent hydrogel biocontainment system for the transformation of inactive chemical compounds prior to coculture experiments. As illustrated in Figure 2A, alginate hydrogel-shell architecture supports a biomimetic milieu where *GUS L. lactis* bacteria were entrapped and shown to grow as colonies producing the GUS enzyme. The microscopic images show *GUS L. lactis* colonies (less than 100 colonies per bead) and continual growth after 3 days of incubation in medium (Figure 2B). The growth of *GUS L. lactis* indicates that small molecules can diffuse freely across the hydrogel shell layer for the active growth of bacterial colonies. For efficient function of bacteria colonies with spatial confinement, it is necessary to evaluate the physiological characteristics of microorganisms such as sustenance, survival, and protein expression in a desired setting. If the confinement space restricts bacteria survival and function, then it could result in low expression of the encoded enzymes upon confinement.[33,35] The hydrogel-shell environment has the potential to effectively contain these bacterial colonies for several days without the disintegration of the shell. The fabrication of the hydrogel shell layer is critical for the integrity of the capsule and to be effective in inhibiting bacteria leakage while the absence of the hydrogel shell could result in leakage of bacteria from the encapsulant with growth (Figure 2C). This is one of the most important characteristics of the hydrogel containment platform for use in prodrug activation experiments. In most cases, the existence of planktonic (free-swimming) uncontrollable bacteria in the growth media could potentially result in spurious results from cancer cell−microbe experiments.

Next, we characterized the physiological characteristics and behavior of bacteria confined in the alginate core−shell beads. The production of bacteria biomass in the bead increased, reaching a phase of maturation until saturation (Figure 2D). The *GUS L. lactis* colonies in the bead environment are subject

https://doi.org/10.1021/acsami.4c02568
ACS Appl. Mater. Interfaces 2024, 16, 28093−28103

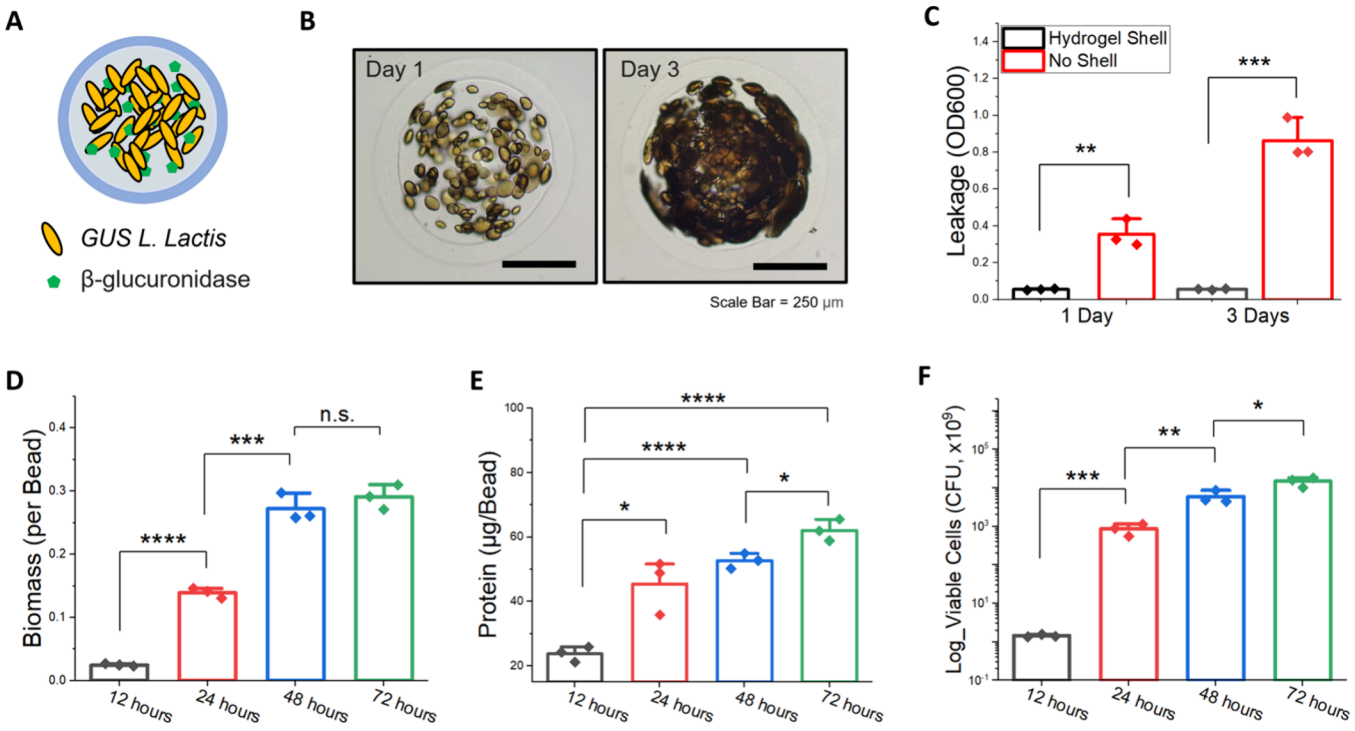

Figure 2. Characterization of hydrogel-shell encapsulation and hydrolysis of glucuronides by β-glucuronidase (GUS) enzyme. (A) Schematic depiction of hydrogel-shell bead encapsulating *GUS L. lactis*. (B) Microscopic images of alginate hydrogel-shell bead with *GUS L. lactis* colonies. Scale bar = 250 μm. (C) Leakage test of bacteria from hydrogel-shell beads by optical density measurement (OD_{600}) in days 1 and 3 with/without constructing a hydrogel shell. (D) Quantification of biomass produced by confined *GUS L. lactis*. (E) Total protein accumulated inside the hydrogel-shell structure. (F) Viable cell counts of hydrogel beads cultivated every 12 h for 3 days, determined by the standard plate method.

to physical constraints when they occupy the rest of the hydrogel core, surrounded by a hydrogel shell layer. Although the physicochemical properties of the hydrogel formation with confined bacterial cells are not completely understood,[34] the confined bacterial colonies formed will gradually be turned into inactive states for long-term survival. During this process, an increased level of total proteins could be observed even after 3 days of incubation since bacterial biomass could be produced by the confined bacteria (Figure 2E). Larger size molecules including enzymes (>25−50 kDa) could accumulate within the polymeric structure as time progresses. In addition, the number of viable *GUS L. lactis* cells continued to increase in the bead environment (Figure 2F). As such, the bacterial GUS enzyme with various metabolic wastes could be produced by *GUS L. lactis* in the polymeric matrices. A range of molecules would be continuously exchanged or accumulated depending on molecular weight and electrostatic interaction in the polymeric environment. Consequently, the amount of biomass with the accumulated protein levels could be proportional to GUS enzymic activity, to result in efficient prodrug activation across the bead system.

Enzymatic Conversion of Substrates. The efficiency of cleavage by the bacteria GUS enzyme is directly associated with the bacteria sustenance and the level of enzyme expression produced upon confinement. To verify the activity of bacterial enzyme as an artificial GUS bioreactor, enzymatic assays were further performed (Figure 3). Glucuronide hydrolysis is an important chemical process for prodrug activation by *GUS L. lactis*.[40] We examined the X-gluc (5-bromo-4-chloro-3-indolyl-β-D-glucuronic acid) dye by the GUS assay to cleave the glucuronide moiety of the chemical structure (Figure 3A and Figure S2). GUS enzyme is synthesized as forming a 75−100 kDa monomer and then the structure of GUS enzyme exists as a 300−400 kDa homotetramer due to structural stability.[40,41] Previous literatures demonstrated the molecular weight cutoff of alginate hydrogels would be around 50−100 kDa.[42,43] The diffusion of high molecular weight proteins could be highly restricted compared with that of low molecular weight molecules in homogeneous hydrogel matrices. Thus, most of the enzymes synthesized from *Lactococcus lactis* colonies could be entrapped in the hydrogel matrices.

The GUS enzyme cleaves the β-glucuronic acid from the X-gluc substrate and produces a blue color product, dichlorodibromo indigo blue. As expected, *GUS L. lactis* beads exhibited a blue color in the solution of X-gluc (Figure 3B). This colorimetric assay indicates the synthesis of GUS enzyme produced by *GUS L. lactis* colonies, to result in an increase of the UV−vis peak in the 630−650 nm range (Figure 3C). However, wild-type *L. lactis* cells colonized within the hydrogel-shell beads were incapable of converting X-gluc into a blue color (absorbance maximum at ∼650 nm) as time progresses through the GUS enzymatic reaction (Figure 3D). Furthermore, we evaluated chemical transformation of GL hydrolysis through liquid chromatography tandem mass spectrometry (LC/MS) analysis[44,45] (Figure 3E,F and Figure S3). The results of the analysis indicate that the GUS enzyme expressed in the hydrogel structures exhibits a significant hydrolysis activity on the glucuronide moiety as the substrates could freely diffuse across the hydrogel polymeric structure. We clearly confirmed enzymatic hydrolysis on the glucuronide moiety in the presence of *GUS L. latics* beads as a functional system for the designed task of pro-apoptotic chemical transformation.

https://doi.org/10.1021/acsami.4c02568
ACS Appl. Mater. Interfaces 2024, 16, 28093−28103

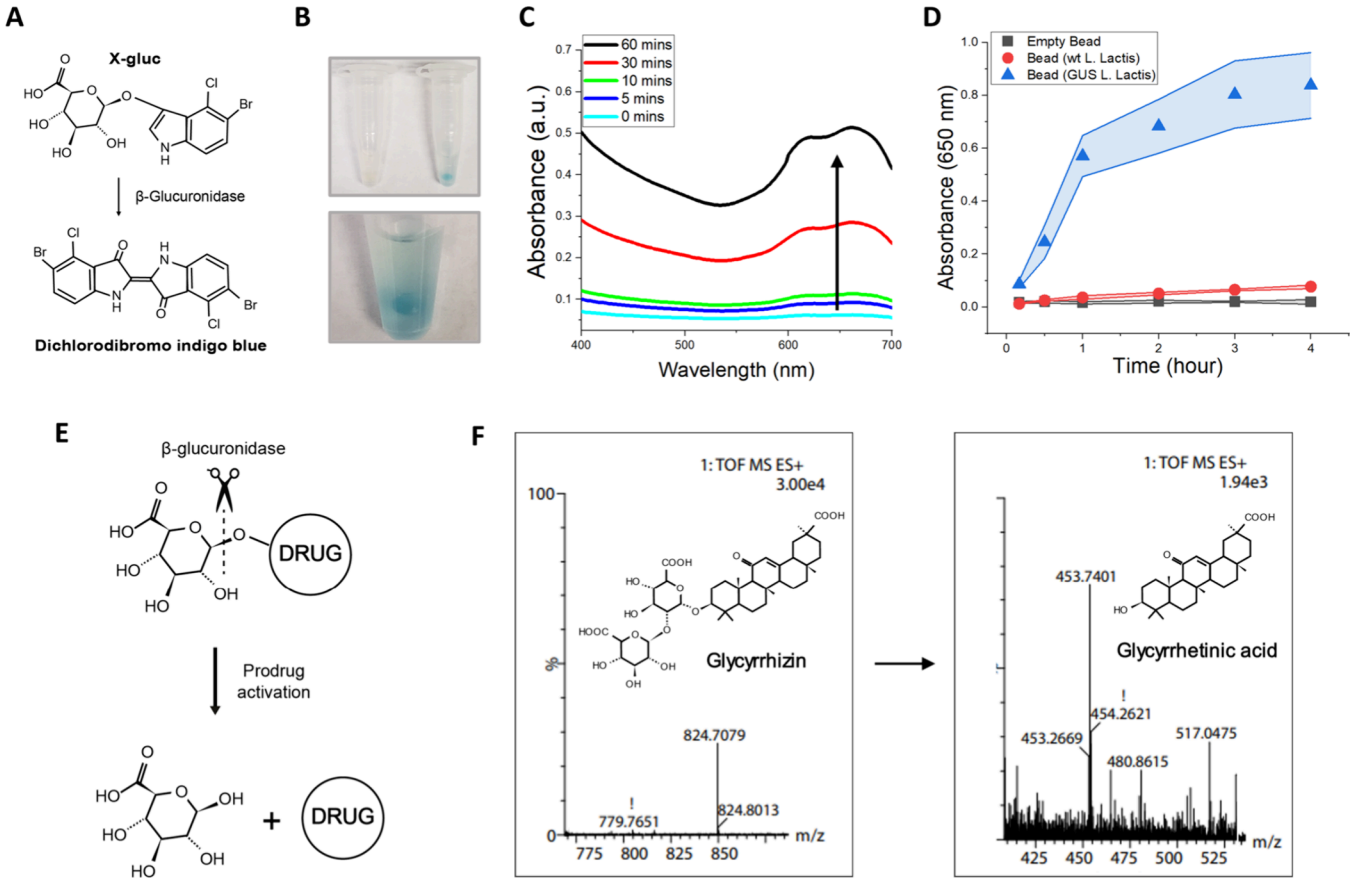

Figure 3. Evaluation of chemical transformation by microbial β-Glucuronidases (GUS) enzyme. (A) Schematic depiction of enzymatic conversion of X-gluc as a substrate of GUS enzyme. (B) Images of color change of the *GUS* activity (upper left: wild-type *L. lactis* hydrogel, upper right: *GUS L. lactis* hydrogel, lower: enlarged image) (C) UV−visible absorption spectra of absorbance changes. (D) Evaluation of *GUS* enzymatic activity responding to *GUS L. lactis* hydrogel incubation with an absorbance maximum at ∼650 nm. * $p < 0.05$, ** $p < 0.01$, *** $p < 0.001$, ***0 *$p <$ 0.0001. Data are mean ± s.d.; $n = 3$ biological replicates. The error band represents the standard deviation of three measurements. (E) Schematic depiction of prodrug activation and glucuronides hydrolysis by microbial β-Glucuronidases (GUS) enzyme. (F) Mass spectra of media samples spiked with chemical structure of glycyrrhizin (GL, glycyrrhizic acid) and glycyrrhetinic acid (GA) (m/z 824 for GL and m/z 453 for GA).

Coculture of 2D Cancer Cells for Prodrug Activation. Exploiting the independent containment of *GUS L. lactis* colonies enables an *in vitro* cocultured environment with cancer cells by controlling the growth of microbes in the system. The basis of this study is the conversion of GL, which comprises glycyrrhetinic acid (GA) and a glucuronide moiety. We hypothesized that the processes of such conversion triggered by bacterial GUS enzyme can improve the therapeutic efficacy of a chemotherapy drug under dynamic coculture conditions.[46,47] As depicted in Figure 4A, we examined whether a natural ingredient of GL could be activated by the bacterial GUS enzyme and evaluated its effect on 2D cancer cells. As stated earlier, one of the major challenges in coculturing bacteria with mammalian cells is in availing a favorable biofilm-like environment for bacteria in cell culture conditions. Bacterial biofilms play a key role in regulating bacteria colonization upon confinement with expression features of enzymes.[33] The microscopic images in Figure 4B show three different types of cancer cells (i.e., HCT116, HepG2, and A498) cultivated in 2D monolayers along with hydrogel-shell beads with *GUS L. lactis* colonies without any leakage after 3 days of coincubation. Herein, encapsulation of microorganisms in the hydrogel matrix has two key roles: The former is the protection of *GUS L. lactis* in a biomimetic condition, and the latter is the prevention of overgrowth to disrupt the system. Some bacterial strains might secrete endogenous toxic compounds such as bacteriocin upon cocultivation with mammalian cells. This implies a possibility that the growth of *GUS L. Lactis* in the hydrogel environment might have adverse effects on the metabolism of cancer cells under coculture conditions. We observed no significant change in cell viability from three tumor cell lines (Figure S4) caused by the secondary metabolites of microbial origin when cocultured with *GUS L. lactis* beads for 48 h.

The natural compound of licorice root, GL is an important product due to its pharmacological properties.[48] For the past years, the pharmacological effects of GL have highlighted the therapeutic feature in its fight against inflammation, neurological diseases, liver diseases, and tumors.[49,50] As hypothesized, we examined the efficacy of the prodrug activation strategy in 2D cell culture by which dose responses with GL alone and GL cocultured with *GUS L. lactis* bead were evaluated from the tumor cell lines (Figure 4C−E). To facilitate comparison across studies, the sensitivity of GL to antitumor effects at a given concentration after exposure to a prodrug treatment (black line) was evaluated. GL dose−response values with the *GUS L. lactis* bead displayed a significant reduction in the effective dose range at the same concentration of GL treatment (red line) (Figure S5). The result of enhanced cytotoxicity in the three types of tumor cells

https://doi.org/10.1021/acsami.4c02568
ACS Appl. Mater. Interfaces 2024, 16, 28093−28103

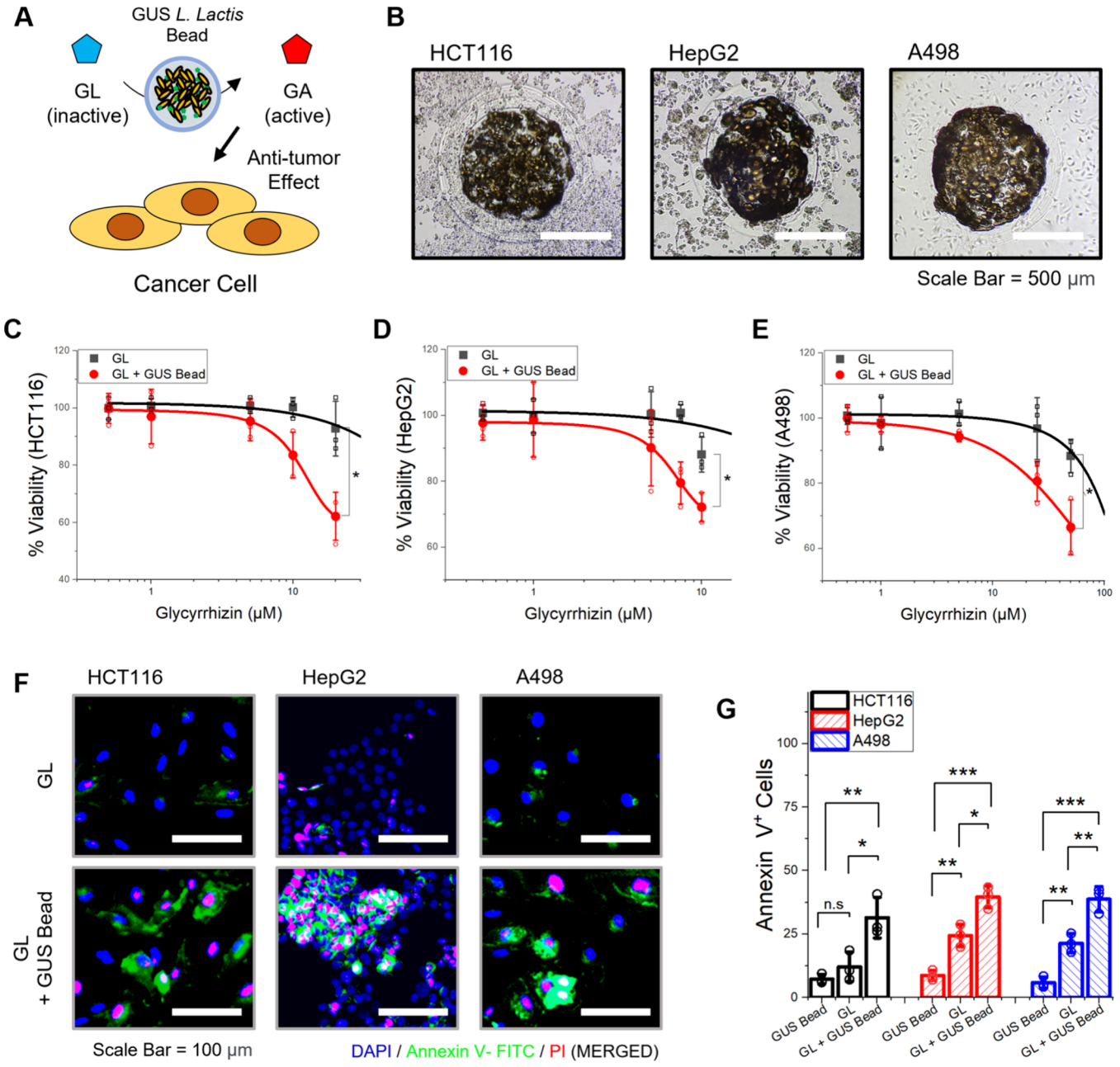

Figure 4. Evaluation of prodrug activation using *in vitro* coculture systems in 2D monolayer culture. (A) Schematic illustration of GL prodrug activation by GUS *L. lactis* hydrogel-shell bead cocultured with human cancer cells. (B) Microscopic images of alginate hydrogel-shell bead with *GUS L. lactis* colonies and cancer cells in monolayer cultures (left to right: HCT116, HepG2 and A498 cells). Scale bar = 500 μm. (C–E) Dose response curve of GL alone (black line and symbols) and GL cocultured with GUS bead (red line and symbols). (F) Annexin V-FITC and PI staining to detect cell apoptosis in the three cell lines cocultured with *GUS L. lactis* bead (GL concentrations: 20 μM for HCT116, 10 μM for HepG2 and 25 μM for A498). Scale bar = 100 μm. (G) Percentage of annexin V positive cells for the quantification of apoptosis induced by GL activation when cocultured with *GUS L. lactis* bead. * $p < 0.05$, ** $p < 0.01$, *** $p < 0.001$, **** $p < 0.0001$. Data are mean ± s.d.; $n = 3$ biological replicates.

could support the claim of chemical transformation of GL by bacterial GUS enzyme to GA. The comparative toxicities of GL and GA have been evaluated in previous mechanistic studies.[51,52] The strong polarity of GL is attributed to the low absorption on the cell membrane resulting in less toxic effects, compared to GA. The reduction of effective GL dose–response due to cytotoxicity underlines the relevant role of the bacterial GUS enzyme due to hydrolysis of β-linked glucuronides to generate active derivatives.

Further, we evaluated the effect of GL activation by the *GUS L. lactis* bead on cell apoptosis through a triple-fluorescence staining method. GA as an active chemical form of GL, has been known to induce cell apoptosis in carcinoma.[53] Fluorescence microscopy revealed that cancer cells underwent apoptosis through GL activation by bacterial GUS enzyme (Figure 4F). Annexin V-FITC and PI signals could barely be detected in the GL treatment groups, but strong fluorescence signals were observed in response to GL treatment with the *GUS L. lactis* bead. Flow cytometry analysis was used to

https://doi.org/10.1021/acsami.4c02568
ACS Appl. Mater. Interfaces 2024, 16, 28093–28103

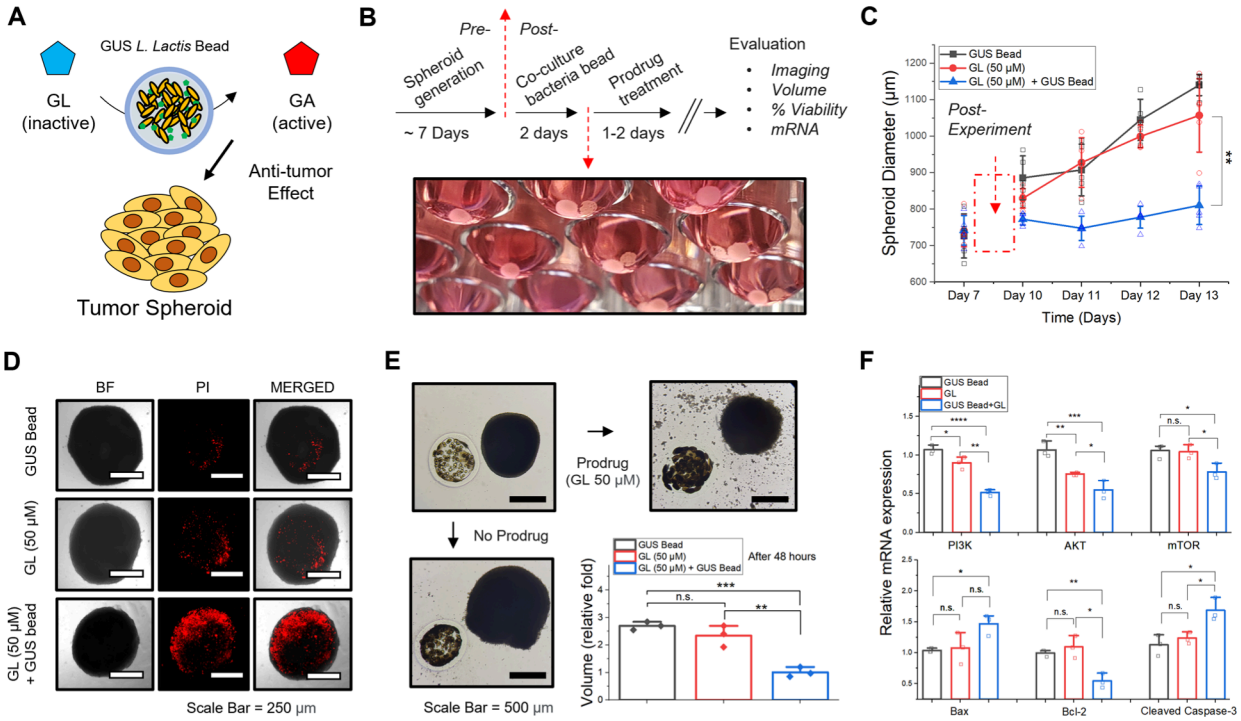

Figure 5. Evaluation of prodrug activation using *in vitro* coculture systems with 3D tumor spheroids. (A) Schematic illustration of GL prodrug activation by *GUS L. lactis* hydrogel-shell bead cocultured with 3D tumor spheroid. (B) Experimental duration for coculture studies with 3D tumor spheroids. Generation of 3D tumor spheroids (for 7 days), cocultured with bacteria bead (2 days) and prodrug treatment (1−2 days) to evaluate GL activation. Imaging, spheroid growth, percentage viability, and mRNA expression were evaluated as analytical end points. Representative images of HCT116 tumor spheroid cocultured with *GUS L. lactis* bead (for next 2 days). (C) Growth monitoring of HCT116 tumor spheroid. (D) Fluorescence microscopic images of stained (PI: propidium iodide) spheroids treated with GL (50 μM) to compare the presence of *GUS L. lactis* hydrogel-shell bead. (E) Images of 3D tumor spheroids with *GUS L. lactis* hydrogel-shell bead and relative spheroid volume upon treatment with GL (50 μM). (F) Relative mRNA expression levels of PI3K, AKT, mTOR, Bcl-2, Bax, and cleaved caspase-3 in 3D tumor spheroid treated with GL (50 μM) to compare the presence of *GUS L. lactis* hydrogel-shell bead. β-actin were used as internal controls. *$p < 0.05$, **$p < 0.01$, *** $p < 0.001$, **** $p < 0.0001$. Data are mean ± s.d.; $n = 3$ biological replicates.

evaluate the degree of GL prodrug activation-induced apoptosis in the cell lines (Figure 4G). In the presence of *GUS L. lactis* bead under coculture conditions, increased numbers of annexin V^+ cells were noted following GL treatment. Our findings are consistent with the data shown above for GL activation by the enzymatic reaction of *GUS L. lactis*. Once GL could be activated by the GUS enzyme, an active chemical form of GA could elevate the therapeutic effect on tumor cells.

Coculture of 3D Tumor Spheroid for Prodrug Activation. We next designed *in vitro* 3D tumor spheroidal cultures with the presence of *GUS L. lactis* beads for the evaluation of prodrug activation. To date, only limited knowledge exists on studies relating to microbial interactions utilizing 3D tumor cultures.[54] Direct administration of microorganism into 3D tumor spheroids have been reported in previous studies.[27] However, such methods through direct inoculation might not be fully applicable for prodrug activation experiments due to the aforementioned challenges of excessive growth or no growth of microorganisms. Past experiments in our laboratory have shown a modified technique for growing 3D tumor spheroids in a contactless environment wherein 3D tumor spheroid cultures could be maintained for an extended period of time in the hanging drop meniscus.[55] As a proof-of-concept, we set out to examine the dynamic interaction of bacteria with the 3D tumor spheroids generated in hanging drop format using a standard 96-well plate (Figure 5A and Figure S6). *In vitro* 3D culture models offer considerable promise because of its physiological relevance in the development and screening of antitumor reagents.[56] In particular, the formation of spheroids enables the replication of cellular heterogeneity in the tumors which results in discrepancy between 2D monolayer and 3D cell cultures to elicit a drug response.[57] Thus, the discrepancy of GL-dose sensitivity in cellular toxicity was evident in 3D tumor cultures compared to 2D monolayer cultured cells (Figure S7).

The experimental steps are listed in Figure 5B. HCT116 3D tumor spheroids were generated in a 96-well plate using the flip hanging drop technique for the first 7 days. A *GUS L. lactis* bead in a hanging drop format could be cocultured for colonization over the next 2 days because GUS enzyme expression is an important step in GL activation in our designed system. During and after growth, *in situ* end point analyses were performed with GL treatment including imaging, fold volume change, percent viability, and mRNA expression of several key genes associated with cell proliferation and apoptotic death in the spheroid samples to verify the enhanced therapeutic effect on 3D tumor spheroids cocultured with *GUS L. lactis*. Formation and growth kinetics of 3D tumor spheroids can be used for the toxicity evaluation of 3D spheroid models. First, spheroid viability assay was performed to evaluate the dose dependent effects of GL activation by the bacterial GUS enzyme (Figure S8). We found that increased toxicity at higher concentration (>50 μM) was noted under these experimental conditions; thus, we examined tumor spheroids under elevated

https://doi.org/10.1021/acsami.4c02568
ACS Appl. Mater. Interfaces 2024, 16, 28093−28103

concentration (50 μM) of GL for prodrug treatment in the following experiments.

Figure 5C shows the growth curves of HCT116 tumor spheroid after 3 days of postexperiments, monitored for 7 days. We observed that the size of the tumor spheroids in the group with GL treatment continued to grow at the same rate as untreated controls. However, the size of the tumor spheroids did not change over time in the group with GL treatment at a 50 μM concentration due to the presence of *GUS L. lactis* beads in 3D cultures. In addition, the results of PI-stained images revealed the obvious death of tumor cells at the edge of spheroids treated with 50 μM of GL and incubated with *GUS L. lactis* bead (Figure 5D). The difference of 3D spheroid volume was nearly 3-fold higher after 48 h of GL treatment between the groups with and without *GUS L. Lactis* bead cocultured for GL activation. As the spheroid formation and morphology changes were observed in the presence of *GUS L. Lactis* bead, the enhanced cytotoxic effect of GL activated by bacteria GUS enzyme was more pronounced (Figure 5E).

To support our hypothesis of prodrug activation, we measured mRNA expression levels in several genes associated with cell proliferation and apoptosis (Figure 5F). The relative mRNA expression level of PI3K, AKT and mTOR was downregulated.[58] The downregulation of the PI3K/AKT/mTOR pathway is associated with inhibition of cell proliferation. Further, the expression of Bax, and cleaved caspase-3 was upregulated, and the expression of Bcl-2 was downregulated in the tumor spheroidal studies. We show that GL activation to GA by the bacteria GUS enzyme inhibits cell proliferation and induces apoptosis. Our findings are consistent and validates the GL activation by *GUS L. lactis* under *in vitro* 3D spheroid coculture models.

CONCLUSION

In summary, we report a coculture strategy for the design of a dynamic *in vitro* interactive platform using hydrogel compartmentalization of microbes, capable of producing microbial GUS enzymes to activate exogenous pharmaceutical compounds by recapitulated microbes. GUS bacterial enzymes produced by *L. lactis* strains provide an important basis for chemotherapeutic prodrug activation, wherein the chemical structure of glycyrrhizin (GL) could be transformed to glycyrrhetinic acid (GA). Based on the conceived system, for the first time, the concept of a systemic enhanced therapeutic response was demonstrated by utilizing conventional 2D tumor cells and 3D tumor spheroids. This presentation focuses on activating prodrug, but the designed tasks would not be limited to activating prodrug. *In vitro* studies are vital for preclinical research given their simplicity yet providing vital information on species interactions in relation to environmental factors. The proposed platform can be used for the construction of complex coculture platforms to query cancer–microbe interactions in a dynamic format to improve our understanding of the interplay of bacteria and host cells and in the evaluation of drug efficacy to develop new therapeutics.

EXPERIMENTAL SECTION

Bacteria Culture. *Lactococcus lactis* NZ9000 *pleiss-Pcon-gusA* (*GUS L. lactis*) was provided by Dr. Lu's group (University of Illinois Urbana–Champaign, Bioengineering).[33] *Lactococcus lactis* subsp. *lactis* (*wild-type L. lactis* ATCC 11454) was obtained from the ATCC (American Type Culture Collection). *GUS L. lactis* was grown in M17 media (HIMEDIA) at 30 °C, and the culture media was supplemented with 0.5% (w/v) glucose and 25 μg/mL of chloramphenicol (Sigma). *L. lactis* ATCC 11454 was grown in brain–heart infusion (BHI) broth (BD Difco) at 37 °C without antibiotics. Bacterial cultures were maintained on a solid agar plate by the addition of 1.5% agar (w/v). Bacteria were cultured overnight on agar plates, and a single colony was inoculated and cultured in the media with shaking. Prior to further experimentation, concentration of bacteria was determined by serial dilution and plating on agar plates to determine colony-forming units (CFU) per mL within 30–300 CFU on a Petri dish.

Hydrogel Core–Shell Structure and Encapsulation of Bacteria. All of the bacteria strains were used without further genetic transformation. Bacteria were prepared overnight on agar plates, and a single colony was picked and inoculated with shaking at 200 rpm in 50 mL of media. Bacteria aliquots were obtained at the exponential growth phase (approximately, $OD_{600} \approx 0.5$ in arbitrary units). The OD value was measured using a UV/vis spectrophotometer (Eppendorf Biophotomer). Bacterial aliquots were resuspended in fresh medium and then mixed with 3 wt % (w/v) of alginate solution prepared in deionized (DI) water. Alginate core hydrogel were fabricated to entrap bacteria at desired cell densities (CFU/mL) by air-extrusion methods as reported.[59] Alginate hydrogels were cross-linked with 0.1 M $CaCl_2$ solution for 10 min. To fabricate a hydrogel-shell layer, the outward gelation method was used as follows; core beads were transferred into a very low concentration of alginate solution (<0.1 wt %) until the final concentration of the alginate solution increased 0.5 wt %. The reaction container was shaken aggressively to prevent agglomeration of core beads. The fabrication steps of a hydrogel-shell layer were controlled by the addition of an excessive amount of DI water. The formed beads with the hydrogel-shell were washed with 0.01 M $CaCl_2$ solution under mild stirring for stabilization and stored in refrigerated conditions at 4 °C until further use.

Hydrogel Stability and Leakage Test. Hydrogel-shell beads with bacterial colonies were observed by using an inverted microscope (Leica DMI3000B) fitted with a CCD camera (Qimaging EXi Blue). The stability of the formed hydrogel beads was monitored every 6 h for 2 days. Bacteria leakage was evaluated in nutritionally complete media. Two groups of *GUS L. lactis* beads with/without a hydrogel shell layer were cultured for 48 h in 10 mL of culture media at 30 °C to test for the leakage of bacteria. The supernatant in each group was measured with a UV/vis spectrophotometer (Eppendorf Biophotomer) every 12 h for 3 days. Stability and bacterial leakage of all hydrogel beads was confirmed in different culture conditions prior to additional coculture experiments.

Biomass and Protein Quantification. Hydrogel-shell beads containing bacterial colonies were collected at each time point. The beads were transferred to a sterilized Eppendorf tube and degraded completely by the addition of 0.1 M sodium citrate solution (Sigma/S4641). Then, bacterial densities and biomass in the bead were estimated by measuring the OD_{600} of the samples. Data set at OD_{600} of the bead samples was recorded for protein measurement. The supernatant of the sample was discarded after centrifugation at 15000 rpm for 3 min. For quantification of intracellular proteins, bicinchoninic acid (BCA) assay (Thermo Scientific) was performed per manufacturer's manuals. Data was normalized against total intracellular protein content with bacterial densities estimated by the previous step.

Viable Cell Count. Hydrogel beads with *GUS L. lactis* colonies were harvested at each time point for viable cell counts. The collected bead samples were degraded completely by the addition of 100 μL of 0.1 M sodium citrate in an Eppendorf tube. Then, 1.4 mL of fresh M17 media was added into the tube, and OD at 600 nm was measured by spectrometry to estimate bacterial densities in the bead. Then, the end point of a bacterial titer (10^{-8}–10^{-12} dilutions) was determined by the standard plate count method on M17 agar plates. All samples on agar plates were incubated at 30 °C. The average colony count between 25 and 150 colonies were considered for plate count after 24 h of incubation.

https://doi.org/10.1021/acsami.4c02568
ACS Appl. Mater. Interfaces 2024, 16, 28093–28103

β-Glucuronidase (GUS) Enzymatic Assays. To examine enzymatic hydrolysis, GUS enzymatic assays were performed using a substrate of X-Gluc (5-bromo-4-chloro-3-indolyl-β-D-glucuronide; Sigma, B5285). Briefly, a stock solution of X-Gluc at a concentration of 10 mM was prepared in DI water. *GUS L. lactis* beads were fabricated by the same method as above. GUS enzymatic assays of hydrogel samples incubated in M17 media were performed by the addition of 10 μL of X-gluc solution. Two groups of hydrogel-shell beads encapsulating either *GUS L. lactis* or *wt L. lactis* were compared as *wt L. lactis* can be a negative control for enzymatic hydrolysis. Dichlorodibromo indigo blue detection with an absorbance maximum at 650 nm was evaluated by spectroscopy. The Synergy H1 multimode plate reader was used to record the absorbance spectra (BioTek).

LC-MS/MS Analysis. Glycyrrhizin (GL, Sigma) was analyzed using the Ultraperformance liquid chromatography mass spectrometry (UPLC-MS) based method, reported previously.[44] *GUS L. lactis* beads were incubated in the media at 50 μM of GL for GUS enzymatic reactions for over 48 h. Culture supernatant of bacteria beads with GL were collected and evaluated by UPLC-MS (Waters Corp, SYNAPT G2-Si system). All samples were evaluated at the School of Chemical Sciences Mass Spectrometry Laboratory (University of Illinois at Urbana−Champaign). The LC separation was performed using a Phenomenex C18 (1.7 μm, 2.1 mm × 50 mm) column, and column temperature was maintained at 40 °C. The mobile phases were used with the solvents A and B for the gradient elution as follows: mobile phase A, 0.4% formic acid in distilled water, and mobile phase B, 5% distilled water in acetonitrile. The following elution condition was used: an isocratic elution with A/B (v/v): 0−0.5 min, 10% B; 0.5:2 min, 10:60% B; 2:3 min, 60:90% B; 3:4 min, 90% B; 4:4.25 min, 90:10% B; 4.25:4.5 min, 10% B. The flow rate was 0.2 mL/min, and the injection volume used was 1 μL. Mass Lynx software v4.1 (Waters Corp) was used to run the experiments, and the chromatogram was analyzed for mass-to-charge ratio (m/z) peaks.

Evaluation of Prodrug Activation by *In Vitro* Coculture Systems. *Coculture of GUS L. lactis Bead in 2D Cancer Cells.* Human cancer cell lines (HCT116, HepG2, and A498) were obtained from the ATCC. HCT116 cells and HepG2 cells were maintained in Dulbecco's modified Eagle's medium (DMEM, Corning) supplemented with 10% fetal bovine serum (FBS, Gibco), supplemented with 1% penicillin/streptomycin (Lonza). A498 cells were grown in Eagle's MEM with L-glutamine (EMEM; ATCC) with 10% fetal bovine serum (FBS, Gibco), supplemented with 1% penicillin/streptomycin (Lonza). WST-1 (Roche Applied Science) assay was performed prior to coculture experiment with *GUS L. lactis* bead to determine the inhibition concentration value of GL.

In vitro 2D coculture studies with *GUS L. lactis* beads were examined for GL prodrug activation. *GUS L. lactis* beads were fabricated to yield bead core diameters of 500 μm and shell layer thickness of 100 μm by the same method.[34] Cancer cells were preincubated without antibiotics in a 48 well plate for 12 h at 37 °C in a humidified incubator, and then *GUS L. lactis* beads were loaded for colonization within the next 48 h. *GUS L. lactis* beads with bacteria growth was observed using an inverted microscope (Leica DMI3000B). After the medium was removed, 300 μL of fresh culture medium containing GL was added. For the cell viability assay, the cytotoxicity of GL at different concentrations was evaluated by the WST-1 assay after 24 h of incubation. Sigmoidal dose−response curves for GL cytotoxicity with/without *GUS L. lactis* bead were generated using Origin 2022 software (Origin Lab). After the indicated GL treatments, cells were stained by the Annexin V-FITC and PI kits (BD Science) for fluorescence microscopy. To identify the cell nucleus, DAPI (Sigma) was used together. Triple stained cells were observed and visualized under a fluorescence microscope (Carl Zeiss Observer Z1). Quantitative analysis of apoptotic cells was determined with a BD LSR II flow cytometer (BD Biosciences). Annexin V-FITC kit (eBiosciences) was used. Data was analyzed with the FCS Express 7 software (De Novo).

Coculture of GUS L. lactis Bead with 3D Tumor Spheroid. For 3D tumor spheroid studies, HCT116 cell lines were used. 3D tumor spheroids were generated by the well-plate flip technique, as reported.[55] After 7 days of incubation in hanging-drop formation, culture media was replenished by manual liquid pipetting, and GL dose response was assessed in 3D spheroids with WST-1 assay. To verify drug discrepancy in 3D tumor cultures at each GL concentration, tumor spheroids were subsequently incubated for 24 h in various concentrations of GL in a 96-well plate without transfer processes and then WST-1 assay for cytotoxicity was performed. Sigmoidal dose−response curves for 2D monolayer culture and 3D tumor spheroid were plotted to compare the GL dose discrepancy.

For coculture studies with *GUS L. lactis* beads, 3D tumor spheroids were prepared for 7 days in a standard 96-well plate with seeding densities of 3×10^3 cells per well. Culture media was replenished, and then *GUS L. lactis* beads were loaded for bacteria colonization for the next 48 h. *GUS L. lactis* bead with 3D tumor spheroid was observed with an inverted microscope (Leica DMI3000B) and photographed using a digital camera. For evaluating GL activation, GL in three different concentrations (20, 50, 100 μM) was examined after 24 or 48 h of incubation. Tumor spheroid proliferation incubated with *GUS L. lactis* bead was measured with WST-1 assay to compare prodrug toxicity at 20, 50, and 100 μM of GL concentration. Post experiments (described in Figure 4B), 3D spheroids were monitored daily and ImageJ software with Fiji macros was used to analyze the size distribution of the tumor spheroids. After GL treatments, the tumor spheroid stained by PI was visualized using a fluorescent microscope (Carl Zeiss Observer Z1).

Total RNA was isolated from tumor spheroid samples using GeneJET RNA Purification Kit (Thermo Fisher Scientific) per manufacturer's manual. Extracted RNA was reverse-transcribed with a High Capacity cDNA Reverse Transcription Kit (Thermo Fisher Scientific) to synthesize cDNA from total RNA. The purity of RNA samples was tested according to the ratio of A_{260nm}/A_{280nm} using a NanoDrop One spectrophotometer (Thermo Fisher Scientific). Primer sequences of all the genes are listed in Supplementary Table 1. Real-time qPCR was performed with a StepOne system (Applied Biosystems). Finally, the expression levels of the target mRNAs were normalized to the reference gene β-actin and calculated as $2^{-\Delta\Delta Ct}$.

Statistical Analysis. All assays and experiments were performed at least in triplicates or more. The data for the experiments was expressed as mean ± standard deviation (s.d.) or violin plot with all the points were obtained. Prism (GraphPad, Ver. 9) was used for statistical analysis using unpaired Student's t test or one-way ANOVA with a post hoc test using the Tukey's method. The details of the statistical tests are presented in each figure legends. The p values with asterisks (<0.05) were considered statistically significant as follows *p < 0.05; **p < 0.01; ***p < 0.001; ****p < 0.0001. No statistical analysis was performed to predetermine a required effect size.

■ ASSOCIATED CONTENT

Supporting Information

The Supporting Information is available free of charge at https://pubs.acs.org/doi/10.1021/acsami.4c02568.

Hydrogel bead, tumor cell death index, and 3D spheroid characterization data (PDF)

■ AUTHOR INFORMATION

Corresponding Author

Joseph Irudayaraj − *Department of Bioengineering, University of Illinois at Urbana−Champaign, Urbana, Illinois 60801, United States; Cancer Center at Illinois, Carle-Illinois College of Medicine, University of Illinois at Urbana−Champaign, Urbana, Illinois 60801, United States; Biomedical Research Center, Mills Breast Cancer Institute, Carle Foundation Hospital, Urbana, Illinois 60801, United States; Carl R. Woese Institute for Genomic Biology, Beckman Institute, Holonyak Micro and Nanotechnology Laboratory, Urbana,*

https://doi.org/10.1021/acsami.4c02568
ACS Appl. Mater. Interfaces 2024, 16, 28093−28103

Illinois 60801, United States; orcid.org/0000-0002-0630-1520; Email: jirudaya@illinois.edu

Authors

Yoon Jeong − *Department of Bioengineering, University of Illinois at Urbana−Champaign, Urbana, Illinois 60801, United States; Cancer Center at Illinois, Carle-Illinois College of Medicine, University of Illinois at Urbana−Champaign, Urbana, Illinois 60801, United States; Biomedical Research Center, Mills Breast Cancer Institute, Carle Foundation Hospital, Urbana, Illinois 60801, United States;* orcid.org/0000-0002-9309-8312

Xiaoxue Han − *Department of Bioengineering, University of Illinois at Urbana−Champaign, Urbana, Illinois 60801, United States; Cancer Center at Illinois, Carle-Illinois College of Medicine, University of Illinois at Urbana−Champaign, Urbana, Illinois 60801, United States; Biomedical Research Center, Mills Breast Cancer Institute, Carle Foundation Hospital, Urbana, Illinois 60801, United States*

Khushali Vyas − *School of Molecular and Cellular Biology, University of Illinois at Urbana−Champaign, Urbana, Illinois 60801, United States*

Complete contact information is available at: https://pubs.acs.org/10.1021/acsami.4c02568

Author Contributions

Y.J.: Conceptualization, Methodology, Investigation, Writing−original draft. X.H.: Investigation, Formal analysis, Writing−review and editing. K.V.: Investigation, Data curation. J.I.: Conceptualization, Funding acquisition, Overall Investigation, Methodology, Project administration, Resources, Supervision, Writing−review and editing.

Notes

The authors declare no competing financial interest.

■ ACKNOWLEDGMENTS

We thank all members of our groups for helpful discussions. This work was supported by the UIUC startup funds to J.I. Partial fellowship support to Y.J. was provided by the National Institute of Biomedical Imaging and Bioengineering of the National Institutes of Health under Award Number T32EB019944. The content is solely the responsibility of the authors and does not necessarily represent the official views of the National Institutes of Health.

■ REFERENCES

(1) Rao, M. B.; Tanksale, A. M.; Ghatge, M. S.; Deshpande, V. V. Molecular and biotechnological aspects of microbial proteases. *Microbiology and molecular biology reviews* **1998**, *62* (3), 597−635.

(2) Johnston, C.; Martin, B.; Fichant, G.; Polard, P.; Claverys, J.-P. Bacterial transformation: distribution, shared mechanisms and divergent control. *Nature Reviews Microbiology* **2014**, *12* (3), 181−196.

(3) Paul, D.; Pandey, G.; Pandey, J.; Jain, R. K. Accessing microbial diversity for bioremediation and environmental restoration. *TRENDS in Biotechnology* **2005**, *23* (3), 135−142.

(4) Gadd, G. M. Biosorption: critical review of scientific rationale, environmental importance and significance for pollution treatment. *Journal of Chemical Technology & Biotechnology: International Research in Process, Environmental & Clean Technology* **2009**, *84* (1), 13−28.

(5) Koppel, N.; Maini Rekdal, V.; Balskus, E. P. Chemical transformation of xenobiotics by the human gut microbiota. *Science* **2017**, *356* (6344), No. eaag2770.

(6) Savage, D. C. Microbial ecology of the gastrointestinal tract. *Annual review of microbiology* **1977**, *31* (1), 107−133.

(7) Rowland, I.; Gibson, G.; Heinken, A.; Scott, K.; Swann, J.; Thiele, I.; Tuohy, K. Gut microbiota functions: metabolism of nutrients and other food components. *European journal of nutrition* **2018**, *57*, 1−24.

(8) Wang, P.; Jia, Y.; Wu, R.; Chen, Z.; Yan, R. Human gut bacterial β-glucuronidase inhibition: An emerging approach to manage medication therapy. *Biochem. Pharmacol.* **2021**, *190*, No. 114566.

(9) Hess, S.; Rambukkana, A. Bacterial-induced cell reprogramming to stem cell-like cells: new premise in host−pathogen interactions. *Curr. Opin. Microbiol.* **2015**, *23*, 179−188.

(10) Qin, S.; Xiao, W.; Zhou, C.; Pu, Q.; Deng, X.; Lan, L.; Liang, H.; Song, X.; Wu, M. Pseudomonas aeruginosa: pathogenesis, virulence factors, antibiotic resistance, interaction with host, technology advances and emerging therapeutics. *Signal Transduction Targeted Ther.* **2022**, *7* (1), 199.

(11) Fuller, R. Probiotics in human medicine. *Gut* **1991**, *32* (4), 439.

(12) Chua, K. J.; Kwok, W. C.; Aggarwal, N.; Sun, T.; Chang, M. W. Designer probiotics for the prevention and treatment of human diseases. *Curr. Opin. Chem. Biol.* **2017**, *40*, 8−16.

(13) Yi, X.; Zhou, H.; Chao, Y.; Xiong, S.; Zhong, J.; Chai, Z.; Yang, K.; Liu, Z. Bacteria-triggered tumor-specific thrombosis to enable potent photothermal immunotherapy of cancer. *Sci. Adv.* **2020**, *6* (33), No. eaba3546.

(14) Sasaki, T.; Fujimori, M.; Hamaji, Y.; Hama, Y.; Ito, K. i.; Amano, J.; Taniguchi, S. i. Genetically engineered Bifidobacterium longum for tumor-targeting enzyme-prodrug therapy of autochthonous mammary tumors in rats. *Cancer science* **2006**, *97* (7), 649−657.

(15) Lehouritis, P.; Springer, C.; Tangney, M. Bacterial-directed enzyme prodrug therapy. *J. Controlled Release* **2013**, *170* (1), 120−131.

(16) Li, N.; Cai, H.; Jiang, L.; Hu, J.; Bains, A.; Hu, J.; Gong, Q.; Luo, K.; Gu, Z. Enzyme-sensitive and amphiphilic PEGylated dendrimer-paclitaxel prodrug-based nanoparticles for enhanced stability and anticancer efficacy. *ACS Appl. Mater. Interfaces* **2017**, *9* (8), 6865−6877.

(17) Zhang, L.; Wang, J.; Cui, H.; Zheng, H.; Yin, X.; Lin, J.; Wang, Y.; Zhao, Y.; Li, H.; Chen, Q. Simultaneous knockdown of immune suppressive markers by tumor microenvironment-responsive multifaceted prodrug nanomedicine. *ACS Appl. Mater. Interfaces* **2023**, *15* (10), 12864−12881.

(18) Li, X.; Ma, Y.; Xin, Y.; Ma, F.; Gao, H. Tumor-targeting nanoassembly for enhanced colorectal cancer therapy by eliminating intratumoral Fusobacterium nucleatum. *ACS Appl. Mater. Interfaces* **2023**, *15* (11), 14164−14172.

(19) Cheng, C.; Lu, Y.; Chuang, K.; Hung, W.; Shiea, J.; Su, Y.; Kao, C.; Chen, B.; Roffler, S.; Cheng, T. Tumor-targeting prodrug-activating bacteria for cancer therapy. *Cancer gene therapy* **2008**, *15* (6), 393−401.

(20) Lehouritis, P.; Stanton, M.; McCarthy, F. O.; Jeavons, M.; Tangney, M. Activation of multiple chemotherapeutic prodrugs by the natural enzymolome of tumour-localised probiotic bacteria. *J. Controlled Release* **2016**, *222*, 9−17.

(21) Chen, G.; Tang, B.; Yang, B.-Y.; Chen, J.-X.; Zhou, J.-H.; Li, J.-H.; Hua, Z.-C. Tumor-targeting Salmonella typhimurium, a natural tool for activation of prodrug 6MePdR and their combination therapy in murine melanoma model. *Applied microbiology and biotechnology* **2013**, *97*, 4393−4401.

(22) Patyar, S.; Joshi, R.; Byrav, D.; Prakash, A.; Medhi, B.; Das, B. Bacteria in cancer therapy: a novel experimental strategy. *J. Biomed. Sci.* **2010**, *17*, 21.

(23) Sedighi, M.; Zahedi Bialvaei, A.; Hamblin, M. R.; Ohadi, E.; Asadi, A.; Halajzadeh, M.; Lohrasbi, V.; Mohammadzadeh, N.; Amiriani, T.; Krutova, M.; et al. Therapeutic bacteria to combat cancer; current advances, challenges, and opportunities. *Cancer Med.* **2019**, *8* (6), 3167−3181.

(24) Di Ventura, B.; Lemerle, C.; Michalodimitrakis, K.; Serrano, L. From in vivo to in silico biology and back. *Nature* **2006**, *443* (7111), 527−533.
(25) Goers, L.; Freemont, P.; Polizzi, K. M. Co-culture systems and technologies: taking synthetic biology to the next level. *Journal of The Royal Society Interface* **2014**, *11* (96), No. 20140065.
(26) Afkhami-Poostchi, A.; Mashreghi, M.; Iranshahi, M.; Matin, M. M. Use of a genetically engineered E. coli overexpressing β-glucuronidase accompanied by glycyrrhizic acid, a natural and anti-inflammatory agent, for directed treatment of colon carcinoma in a mouse model. *Int. J. Pharm.* **2020**, *579*, No. 119159.
(27) Kasper, S. H.; Morell-Perez, C.; Wyche, T. P.; Sana, T. R.; Lieberman, L. A.; Hett, E. C. Colorectal cancer-associated anaerobic bacteria proliferate in tumor spheroids and alter the microenvironment. *Sci. Rep.* **2020**, *10* (1), 5321.
(28) Zhao, M.; Yang, M.; Li, X.-M.; Jiang, P.; Baranov, E.; Li, S.; Xu, M.; Penman, S.; Hoffman, R. M. Tumor-targeting bacterial therapy with amino acid auxotrophs of GFP-expressing Salmonella typhimurium. *Proc. Natl. Acad. Sci. U. S. A.* **2005**, *102* (3), 755−760.
(29) Wang, D.; Liu, C.; You, S.; Zhang, K.; Li, M.; Cao, Y.; Wang, C.; Dong, H.; Zhang, X. Bacterial vesicle-cancer cell hybrid membrane-coated nanoparticles for tumor specific immune activation and photothermal therapy. *ACS Appl. Mater. Interfaces* **2020**, *12* (37), 41138−41147.
(30) Gao, Z.; Zhang, E.; Zhao, H.; Xia, S.; Bai, H.; Huang, Y.; Lv, F.; Liu, L.; Wang, S. Bacteria-mediated intracellular click reaction for drug enrichment and selective apoptosis of drug-resistant tumor cells. *ACS Appl. Mater. Interfaces* **2022**, *14* (10), 12106−12115.
(31) Song, J.; Zhang, Y.; Zhang, C.; Du, X.; Guo, Z.; Kuang, Y.; Wang, Y.; Wu, P.; Zou, K.; Zou, L.; et al. A microfluidic device for studying chemotaxis mechanism of bacterial cancer targeting. *Sci. Rep.* **2018**, *8* (1), 6394.
(32) Kim, J.; Hegde, M.; Jayaraman, A. Co-culture of epithelial cells and bacteria for investigating host−pathogen interactions. *Lab Chip* **2010**, *10* (1), 43−50.
(33) Jeong, Y.; Kong, W.; Lu, T.; Irudayaraj, J. Soft hydrogel-shell confinement systems as bacteria-based bioactuators and biosensors. *Biosens. Bioelectron.* **2023**, *219*, No. 114809.
(34) Jeong, Y.; Irudayaraj, J. Hierarchical Encapsulation of Bacteria in Functional Hydrogel Beads for Inter-and Intra-species Communication. *Acta Biomaterialia* **2023**, *158*, 203−215.
(35) Jeong, Y.; Ahmad, S.; Irudayaraj, J. Dynamic Effect of β-Lactam Antibiotic Inactivation Due to the Inter-and Intraspecies Interaction of Drug-Resistant Microbes. *ACS Biomaterials Science & Engineering* **2024**, *10* (3), 1461−1472.
(36) Dabek, M.; McCrae, S. I.; Stevens, V. J.; Duncan, S. H.; Louis, P. Distribution of β-glucosidase and β-glucuronidase activity and of β-glucuronidase gene gus in human colonic bacteria. *FEMS microbiology ecology* **2008**, *66* (3), 487−495.
(37) Gao, S.; Sun, R.; Singh, R.; Yu So, S.; Chan, C. T.Y.; Savidge, T.; Hu, M. The role of gut microbial β-glucuronidase in drug disposition and development. *Drug Discovery Today* **2022**, *27* (10), No. 103316.
(38) Cinatl, J.; Morgenstern, B.; Bauer, G.; Chandra, P.; Rabenau, H.; Doerr, H. Glycyrrhizin, an active component of liquorice roots, and replication of SARS-associated coronavirus. *Lancet* **2003**, *361* (9374), 2045−2046.
(39) Jeong, Y.; Vyas, K.; Irudayaraj, J. Toxicity of per-and polyfluoroalkyl substances to microorganisms in confined hydrogel structures. *Journal of hazardous materials* **2023**, *456*, No. 131672.
(40) Hull, G. A.; Devic, M. The β-glucuronidase (gus) reporter gene system: gene fusions; spectrophotometric, fluorometric, and histochemical detection. *Plant Gene transfer and expression protocols* **1995**, *49*, 125−141.
(41) Swank, R. T.; Paigen, K. Biochemical and genetic evidence for a macromolecular β-glucuronidase complex in microsomal membranes. *J. Mol. Biol.* **1973**, *77* (3), 371−389.
(42) Augst, A. D.; Kong, H. J.; Mooney, D. J. Alginate hydrogels as biomaterials. *Macromol. Biosci.* **2006**, *6* (8), 623−633.
(43) Lee, K. Y.; Mooney, D. J. Alginate: properties and biomedical applications. *Prog. Polym. Sci.* **2012**, *37* (1), 106−126.
(44) Xu, T.; Yang, M.; Li, Y.; Chen, X.; Wang, Q.; Deng, W.; Pang, X.; Yu, K.; Jiang, B.; Guan, S.; et al. An integrated exact mass spectrometric strategy for comprehensive and rapid characterization of phenolic compounds in licorice. *Rapid Commun. Mass Spectrom.* **2013**, *27* (21), 2297−2309.
(45) Lin, Z. J.; Qiu, S.-X.; Wufuer, A.; Shum, L. Simultaneous determination of glycyrrhizin, a marker component in radix Glycyrrhizae, and its major metabolite glycyrrhetic acid in human plasma by LC−MS/MS. *Journal of Chromatography B* **2005**, *814* (2), 201−207.
(46) Dashnyam, P.; Mudunuddla, R.; Hsieh, T.-J.; Lin, T.-C.; Lin, H.-Y.; Chen, P.-Y.; Hsu, C.-Y.; Lin, C.-H. β-Glucuronidases of opportunistic bacteria are the major contributors to xenobiotic-induced toxicity in the gut. *Sci. Rep.* **2018**, *8* (1), No. 16372.
(47) Zou, S.; Liu, G.; Kaleem, I.; Li, C. Purification and characterization of a highly selective glycyrrhizin-hydrolyzing β-glucuronidase from Penicillium purpurogenum Li-3. *Process Biochemistry* **2013**, *48* (2), 358−363.
(48) Isbrucker, R.; Burdock, G. Risk and safety assessment on the consumption of Licorice root (Glycyrrhiza sp.), its extract and powder as a food ingredient, with emphasis on the pharmacology and toxicology of glycyrrhizin. *Regul. Toxicol. Pharmacol.* **2006**, *46* (3), 167−192.
(49) Wang, Z. Y.; Nixon, D. W. Licorice and cancer. *Nutrition and cancer* **2001**, *39* (1), 1−11.
(50) Su, X.; Wu, L.; Hu, M.; Dong, W.; Xu, M.; Zhang, P. Glycyrrhizic acid: A promising carrier material for anticancer therapy. *Biomedicine & Pharmacotherapy* **2017**, *95*, 670−678.
(51) Final report on the safety assessment of glycyrrhetinic acid, potassium glycyrrhetinate, disodium succinoyl glycyrrhetinate, glyceryl glycyrrhetinate, glycyrrhetinyl stearate, stearyl glycyrrhetinate, glycyrrhizic acid, ammonium glycyrrhizate, dipotassium glycyrrhizate, disodium glycyrrhizate, trisodium glycyrrhizate, methyl glycyrrhizate, and potassium glycyrrhizinate. *Int. J. Toxicol.* **2007**, *26*, 79−112,.
(52) Xu, Y.; Feng, X.; Jia, J.; Chen, X.; Jiang, T.; Rasool, A.; Lv, B.; Qu, L.; Li, C. A novel β-glucuronidase from Talaromyces pinophilus Li-93 precisely hydrolyzes glycyrrhizin into glycyrrhetinic acid 3-O-mono-β-d-glucuronide. *Appl. Environ. Microbiol.* **2018**, *84* (19), e00755-18.
(53) Satomi, Y.; Nishino, H.; Shibata, S. Glycyrrhetinic acid and related compounds induce G1 arrest and apoptosis in human hepatocellular carcinoma HepG2. *Anticancer Res.* **2005**, *25* (6B), 4043−4047.
(54) Osswald, A.; Sun, Z.; Grimm, V.; Ampem, G.; Riegel, K.; Westendorf, A. M.; Sommergruber, W.; Otte, K.; Dürre, P.; Riedel, C. U. Three-dimensional tumor spheroids for in vitro analysis of bacteria as gene delivery vectors in tumor therapy. *Microb. Cell Fact.* **2015**, *14*, 199.
(55) Jeong, Y.; Tin, A.; Irudayaraj, J. Flipped Well-Plate Hanging-Drop Technique for Growing Three-Dimensional Tumors. *Frontiers in Bioengineering and Biotechnology* **2022**, *10*, No. 898699.
(56) Costa, E. C.; Moreira, A. F.; de Melo-Diogo, D.; Gaspar, V. M.; Carvalho, M. P.; Correia, I. J. 3D tumor spheroids: an overview on the tools and techniques used for their analysis. *Biotechnology advances* **2016**, *34* (8), 1427−1441.
(57) Riedl, A.; Schlederer, M.; Pudelko, K.; Stadler, M.; Walter, S.; Unterleuthner, D.; Unger, C.; Kramer, N.; Hengstschläger, M.; Kenner, L. Comparison of cancer cells in 2D vs 3D culture reveals differences in AKT−mTOR−S6K signaling and drug responses. *J. Cell Sci.* **2017**, *130* (1), 203−218.
(58) Riquelme, I.; Tapia, O.; Espinoza, J. A.; Leal, P.; Buchegger, K.; Sandoval, A.; Bizama, C.; Araya, J. C.; Peek, R. M.; Roa, J. C. The gene expression status of the PI3K/AKT/mTOR pathway in gastric cancer tissues and cell lines. *Pathology & Oncology Research* **2016**, *22* (4), 797−805.

https://doi.org/10.1021/acsami.4c02568
ACS Appl. Mater. Interfaces 2024, 16, 28093−28103

(59) Jeong, Y.; Irudayaraj, J. Multi-layered alginate hydrogel structures and bacteria encapsulation. *Chem. Commun.* **2022**, *58* (61), 8584−8587.

https://doi.org/10.1021/acsami.4c02568
ACS Appl. Mater. Interfaces 2024, 16, 28093−28103